



DETERMINATION OF SLIP-RATE BY OPTICAL DATING OF LAKE BED SEDIMENTS FROM THE DASHT-E-BAYAZ FAULT, NE IRAN

MORTEZA FATTAHI^{1,2}, RICHARD WALKER³, MOHAMMAD M KHATIB⁴,
MOHAMMAD ZARRINKOUB⁴ and MORTEZA TALEBIAN⁵

¹*Institute of Geophysics, Tehran University, Kargar Shomali, Tehran, Iran.*

²*The School of Geography, University of Oxford, south park road, Oxford OX1 3QY, UK*

³*Department of Earth Sciences, University of Oxford, Parks Road, Oxford OX1 3AN, UK*

⁴*Department of geology, Birjand University, P.o.Box 131, Birjand, Iran.*

⁵*Geological Survey of Iran, Azadi Square, Meraj Avenue, P.O. Box 11365-4563, Tehran, Iran*

Received 27 September 2014

Accepted 9 April 2015

Abstract: The Dasht-e-Bayaz left-lateral strike-slip fault in northeastern Iran ruptured in two destructive earthquakes in 1968 and 1979. The western half of the Dasht-e-Bayaz fault cuts across the dry lake-bed in the Nimbluk valley and has no measurable relief except for a few localised jogs in the fault trace. We provide the first quantitative constraint on the slip-rate of the Dasht-e-Bayaz fault averaged over the Holocene. The western part of the fault cuts across the Nimbluk valley; the flat surface of which is composed of lake-bed sediments. Small streams cut into the surface of the lake-beds are displaced across the fault by 26 ± 2 m. Two OSL samples of the lake-bed sediments are successfully dated at 8.6 ± 0.6 and 8.5 ± 1.0 ka, from which we calculate a minimum slip-rate of 2.6 mm/yr. This minimum slip rate remains constant with the previously proposed Holocene slip rate of 2.5 mm/yr and within the range of the Holocene slip rate of 2.4 ± 0.3 mm/yr estimated before on the central section of the Doruneh fault.

Keywords: slip-rate, OSL, Dasht-e-Bayaz fault, NE Iran.

1. INTRODUCTION

On the 30 August 1968, the western 80 km of the left-lateral Dasht-e-Bayaz fault in northeastern Iran ruptured in an earthquake of Mw 7.1 that killed an estimated 7000 to 12000 people (e.g., Ambraseys and Tchalenko, 1969; Tchalenko and Ambraseys, 1970; Tchalenko and Berberian, 1975; Walker *et al.*, 2004; Walker *et al.*, 2011). In the thirty years following 1968 the Dasht-e-Bayaz and Zirkuh region has been subject to numerous further earthquakes, including four events of Mw 5.5-6, four

events of Mw 6-7, and a further two events of Mw 7.1. The first of these two Mw 7.1 earthquakes, (the 10 May 1997 Zirkuh earthquake) ruptured the north-south right-lateral Abiz fault (**Fig. 1b**). The second (the Khulibuniabad earthquake of the 27 November 1979), ruptured the eastern 60 km of the Dasht-e-Bayaz fault (**Fig. 1b**) from west of Zigan village in the west to Buniabad in the east (e.g. Haghypour and Amidi, 1980; Nowroozi and Mohajer-Ashjai, 1980; Walker *et al.*, 2011). The earthquake apparently re-ruptured the eastern 10 km of the surface breaks generated during the 1968 Dasht-e-Bayaz earthquake (Ambraseys and Tchalenko, 1969).

Together, the sequence of eleven earthquakes within 30 years at Dasht-e-Bayaz and Zirkuh region forms one of the most outstanding examples of clustered large-magnitude seismic activity in the world (e.g. Berberian *et*

Corresponding author: M. Fattahi
e-mail: mfattahi@ut.ac.ir

al. 1999; Berberian and Yeats 1999a; Berberian, 1976; Walker *et al.*, 2011), of which two of these earthquakes were occurred on the Dasht-e-Bayaz fault itself. Walker *et al.* (2011) performed a multiple-event relocation analysis, using calibrated relocations, InSAR and high-resolution satellite imagery, to better image the distribution of seismicity within the Dasht-e-Bayaz and Zirkuh region of northeastern Iran. Their study confirmed that the 30 August 1968 M_w 7.1 Dasht-e-Bayaz earthquake nucleated at a prominent segment boundary and left-step in the fault trace, and that the 11 September 1968 M_w 5.6 aftershock occurred on the Dasht-e-Bayaz fault at the eastern end of the 1968 rupture (see Fig. 4 of Walker *et al.*, 2011).

Determining the slip rate and the recurrence interval between large events on the Dasht-e-Bayaz fault is of importance for estimating the hazard posed by the fault to local populations and also for the more general issue of the clustering in time of large earthquake events.

In this paper, we provide the first quantitative fault slip-rate estimate for the Dasht-e-Bayaz fault from optically stimulated luminescence (OSL) dating of lake-bed sediments displaced by the fault. Our data can be used to determine an average recurrence interval for earthquakes such as the 1968 and 1979 events (with strike-slip displacements of up to 4.5 m and 4 m, respectively). Our results also can be used to provide valuable constraints for understanding the role of the Dasht-e-Bayaz fault in the accommodation of tectonic strain in northeast Iran.

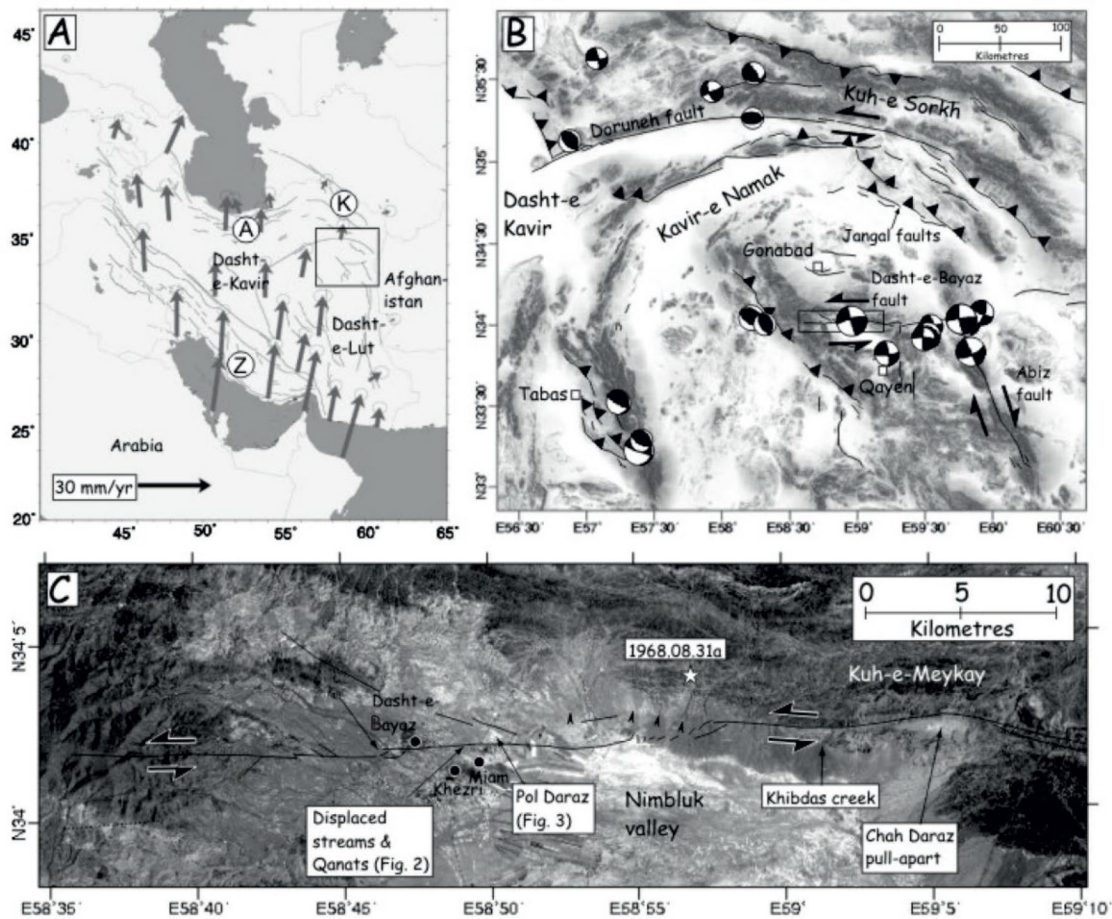


Fig. 1. (a) Map of Iran with GPS velocities of points relative to Eurasia from Vernant *et al.* (2004). Z = Zagros; A = Alborz; K = Kopeh Dagh. (b) Shaded-relief topographic map of the Dasht-e-Bayaz region (SRTM topography; Farr and Kobrick, 2000). Fault-plane solutions of major earthquakes are from waveform modelling (listed in Jackson, 2001) and the Harvard CMT catalogue (<http://www.globalcmt.org/>). (c) ASTER satellite image of the western Dasht-e-Bayaz fault with ruptures of the 1968 earthquake (Ambraseys and Tchalenko, 1969; Tchalenko and Ambraseys, 1970; Tchalenko and Berberian, 1975; Berberian, 1976). The epicentre of the 1968 earthquake is marked by a white star (Engdahl *et al.*, 1998). The location of displaced streams and Qanats (Fig. 2) and the Pol Daraz sampling site (Figs. 3 and 4) are labelled. (A and B are in a Mercator projection, C is in UTM40 projection).

2. ACTIVE TECTONICS OF THE DASHT-E-BAYAZ REGION

The active tectonics of Iran are controlled by the northward motion of Arabia relative to Eurasia (Fig. 1a; Vernant *et al.*, 2004). The GPS velocities of points relative to Eurasia decrease to zero at both the northern and eastern borders of Iran indicating that the major part of the continental shortening is confined within the political borders of Iran, with the majority of the deformation concentrated in the Zagros mountains of southern Iran (Z in Fig. 1a), and in the Alborz and Kopeh Dagh mountains in the north (A and K in Fig. 1a). The arid interior of Iran (Dasht-e-Kavir, Fig. 1a) is virtually aseismic and appears to not be deforming as rapidly as its surroundings.

The rate of present-day northward movement of Central Iran with respect to stable Eurasia and, therefore, the right-lateral shear between Central Iran and Eurasia is less than 16 ± 2 mm/yr (Walpersdorf *et al.*, 2014). South of latitude 34°N this shear is accommodated on north-south right-lateral faults that surround the Dasht-e-Lut (e.g. Walker and Jackson, 2004; Meyer and Le Dortz, 2007; see Fig. 1a). North of latitude 34°N , however, the shear is accommodated by east-west, left-lateral, faults that are thought to rotate clockwise about a vertical axis (Jackson and McKenzie, 1984). The most prominent of the left-lateral faults are the Doruneh and Dasht-e-Bayaz faults (Fig. 1b).

Walker *et al.* (2004) suggest, from the relatively small total displacement across the Dasht-e-Bayaz fault of $\sim 4\text{--}5$ km, that the Dasht-e-Bayaz fault is a relatively young feature. They further suggest that the Dasht-e-Bayaz fault has formed in response to the accommodation of large amounts of slip, and large amounts of vertical axis rotation, that have caused the Doruneh fault to become oriented in a direction that is non-optimal for continued movement. To test whether the Dasht-e-Bayaz is presently the more active of the two faults requires estimates of the slip-rate on both.

Fattahi *et al.* (2007) determined a slip-rate on the Doruneh fault of 2.4 ± 0.3 mm/yr averaged over the Holocene using Infra-red stimulated luminescence (IRSL) dating of feldspar grains from incised alluvial fan deposits displaced by faulting. The only existing constraint on the slip-rate of the Dasht-e-Bayaz fault is that it is believed to be in excess of 2.5 mm/yr based on assumptions about the age of a series of Qanats (underground irrigation canals) displaced left-laterally by ~ 10 m across the fault (Ambraseys and Tchalenko, 1969; Berberian and Yeats, 1999b; Walker *et al.*, 2004, also see Fig. 2b).

3. MEASURING THE SLIP-RATE OF THE DASHT-E-BAYAZ FAULT

A major difficulty in measuring slip-rate on the Dasht-e-Bayaz fault is the overall lack of relief across it. The western half of the Dasht-e-Bayaz fault cuts across a

dry lake-bed in the Nimbluk valley and has no measurable relief except for at a few localised jogs in the fault trace (Fig. 1c). As Quaternary slip-rate estimates on strike-slip faults generally rely on the identification of landforms of known age that have been displaced by fault movement (e.g. Ritz *et al.*, 1995; Van Der Woerd *et al.*, 2006; Fattahi *et al.*, 2006) the estimation of slip-rate on the Dasht-e-Bayaz fault poses a considerable challenge.

In the following section we describe drainage features, observed within the Nimbluk valley, which show cumulative left-lateral displacements of several tens of metres. We then apply the age of the Nimbluk dry lake, using OSL dating of the lake-bed sediments, to determine a rate of slip for the Dasht-e-Bayaz fault.

Stream offsets on the Nimbluk dry lake-bed

Fig. 2a is an aerial photograph, taken in 1968, showing a part of the Dasht-e-Bayaz earthquake ruptures tracking across the Nimbluk dry lake-bed (reproduced from Ambraseys and Tchalenko, 1969). A scale has been assigned to the aerial photograph by overlaying it with Quickbird satellite imagery obtained from GoogleEarth (<http://earth.google.com/>). Distortion across the small area of the photograph represented in Fig. 2a is negligible. The trace of the Dasht-e-Bayaz fault, and many of the stream channels displaced across it (see below), have been eradicated by extensive farming (Fig. 3) over the past forty years and are unidentifiable either in the field or in Quickbird imagery. The information preserved within the aerial photograph thus provides our only reliable method of identifying cumulative displacements.

A series of slightly incised southeast-flowing streams cross the surface of the Nimbluk valley (Fig. 2a). Where these streams cross the trace of the Dasht-e-Bayaz fault they appear to be deflected in a left-lateral sense. The measurement of the horizontal displacement is affected by uncertainties, such as: 1) the original watercourse was not necessarily straight, as suggested by different crossing angles between the upstream and the downstream reaches at the fault; and 2) erosion due to fluvial processes that can overcome the tectonic signal by straightening the stream course.

Figs. 2b to 2d are detailed geomorphic maps of three of the apparent stream deflections. Note that in each of these panels the Dasht-e-Bayaz fault zone has a north-south width of several tens of metres and we therefore measure the displacement across this entire zone. In all cases, the displacements are measured from the centre of the stream channels.

A fourth stream visible in Fig. 2a shows no clear displacement apart from the ~ 3 m of co-seismic slip in the 1968 earthquake. The lack of any deflection could be due to its stronger stream power to straighten the course and erase the offset.

The most westerly of the three streams (Fig. 2b) enters the fault zone with a linear SSE-trending channel. It then bends to the east before exiting the fault zone with a

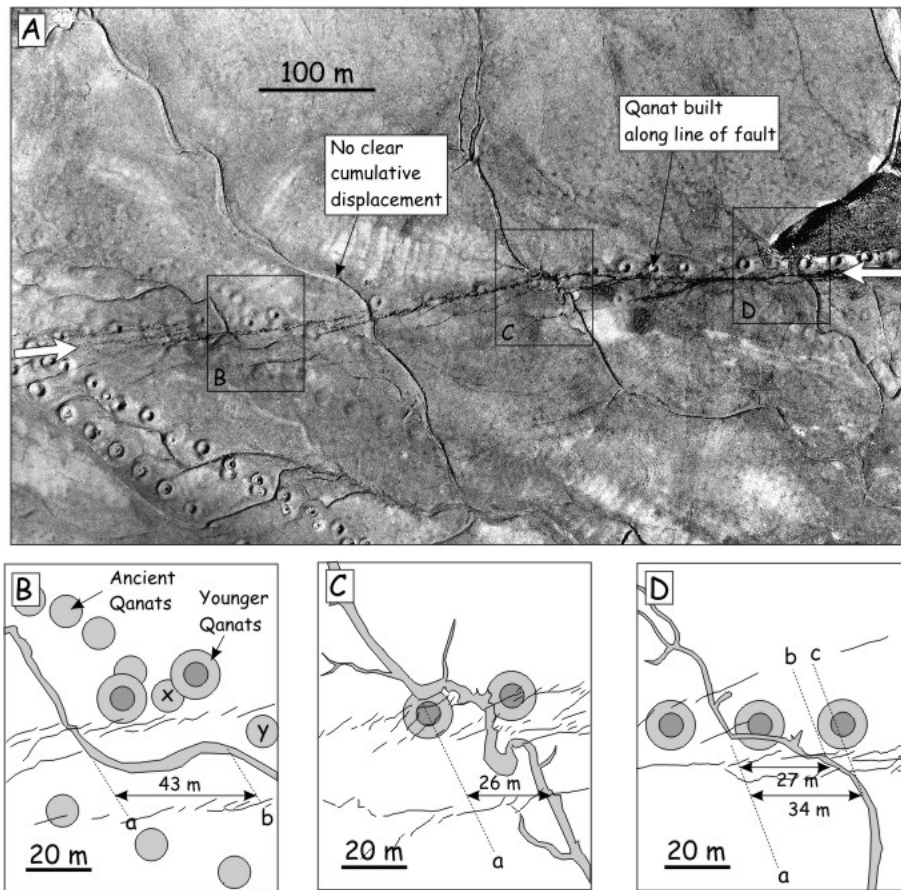


Fig. 2. (a) Aerial photograph of the 1968 Dasht-e-Bayaz earthquake ruptures north of Khezri (photograph is reproduced from Ambraseys and Tchalenko, 1969) $\sim 34.03418^{\circ}\text{N}$; 58.82130°E . The ruptures run east to west between the white arrows. Scale was calculated by overlaying high-resolution Quickbird imagery from GoogleEarth (<http://earth.google.com/>). The three boxes cover the regions represented in panels b, c and d. (b) Map of drainage and qanat systems displaced by faulting. A line of ancient, heavily eroded, qanat tunnels is apparently displaced by ~ 10 m across the fault (between points x and y). The second line of ancient qanats, which tracks across the southwest corner of the image, is also displaced by ~ 10 m at the fault (Ambraseys and Tchalenko, 1969). The apparent stream displacement of >43 m is probably not real (see text). (c and d) Maps showing cumulative displacement of another two streams. In (c) a linear, southeast-flowing, stream is displaced by 26 ± 2 m. In (d) the stream is left-laterally displaced by 27 ± 2 m across the fault zone (correlation between lines a and b). However, if parallel, southeast-flowing, parts of the stream course are correlated the total displacement could be 34 m. Among these displacements the 26 ± 2 m displacement seems to be the most reliable because the channel of that stream is very straight and narrow. For the measurement of this displacement an uncertainty of ± 2 m is assigned.

southeast flow direction. Extrapolation of the SSE-trending part of the stream channel (line 'a'), to the bend from east-trending to southeast-trending parts of the channel (line 'b'), provides an estimate of greater than 43 m of left-lateral displacement. The stream does not have a linear SSE-trending channel at both sides of the fault zone. The eastward-flowing portion of the channel is parallel to the margins of the fault zone in which it is situated (Fig. 2b). The stream course appears to be influenced by the fault and is therefore not a passive marker of cumulative fault displacement. Two lines of eroded, and presumably ancient, Qanat systems are visible in Fig. 2b. These two Qanats are displaced by ~ 10 m across the fault

zone (Ambraseys and Tchalenko, 1969). The displacement of one of the Qanat systems is visible in Fig. 2b (between points x and y). If we can date the Qanat, then it is possible to find an slip rate using Qanat displacement.

The displacement of the central stream (Fig. 2c) is much clearer. The stream has a linear SSE-trending channel at both sides of the fault zone. Within the fault zone the channel is highly disrupted. Correlation of the centre of the two SSE-trending stream courses provides a cumulative left-lateral displacement of 26 ± 2 m. The extremely straight, and parallel, stream courses on both sides of the fault give us confidence that the 26 ± 2 m reflects a true cumulative displacement across the fault.



Fig. 3. The trace of the Dasht-e-Bayaz fault, and many of the stream channels displaced across it, have been eradicated by extensive farming and transferring the lake bed sediments to somewhere else.

The eastern stream (Fig. 2d) has a SSE trend where it enters the fault zone. It then abruptly bends to an easterly course. It then gently curves round to a southerly course as it exits the fault zone. Correlation of the linear SSE-trending part of the channel (line ‘a’) with the most easterly part of the course south of the fault (line ‘c’) provides an estimate of displacement of 34 m with greater than ± 2 m uncertainty. However, correlation with the location of the stream channel as it exits the fault zone (line ‘b’) provides a displacement of 27 ± 2 m. The cumulative displacement is therefore at least 27 ± 2 m and may be higher.

Taken together, the three displaced streams show that at least 26 ± 2 m of left-lateral displacement has occurred across the Dasht-e-Bayaz fault since desiccation of the Nimbluk palaeo-lake. The central of the three streams, from which the measurement of 26 ± 2 m comes from, is the most convincing of the three displacement measurements. This value also agrees with the measurements of Berberian and Yeats (1999a) who note several streams along the Dasht-e-Bayaz fault with cumulative displace-

ments of 8–28 m. We do not, however, rule out that larger amounts of displacement have occurred since lake desiccation. The measurement of 26 ± 2 m should, therefore, be considered to be a minimum estimate of slip. The stream systems are cut into the surface of a dry lake-bed and must postdate desiccation of the Nimbluk palaeo-lake. Constraints on the age of lake-bed deposition will thus allow us to estimate a minimum rate of slip on the Dasht-e-Bayaz fault.

Optically-stimulated luminescence (OSL) dating of lake-bed sediments

North of Khezri, immediately to the east of the main Qayen to Gonabad road sediments of the Nimbluk palaeo-lake are exposed at Pol Daraz (Fig. 4a). Pol Daraz has been uplifted by a small component of vertical slip on the Dasht-e-Bayaz fault (Fig. 4b). Two samples of lake-bed sediments exposed at Pol Daraz were extracted from vertical exposures of fine-grained and homogeneous lake-bed sediments. Fig. 4c shows the position of DB1 sample (34:02:02.4N; 58:49:56.6E; Altitude 1540 m) which was taken as a single block of lake-bed sediments (Fig. 4c). The sample was wrapped by aluminium foil and covered by black plastic bag. The other OSL sample (DB2) was taken by metal tube, from 34:02:04.0N; 58:49:51.2E; 1554 m.

Under subdued red light in the laboratory, the outside, light exposed, parts of the block sample, DB1, were trimmed and removed. Two centimetres from both ends of the tube sample, DB2, which could be exposed to light was separated and used for moisture measurement. The rest was used for equivalent dose determination. A portion of both samples were wet-sieved to separate the 90–150 μm grains and immersed for two days in 1 N HCl to remove carbonate, followed by one day immersion in H_2O_2 to remove organic material. Heavy minerals (density $> 2.72 \text{ g cm}^{-3}$) were removed from the treated sample fraction by heavy liquid (sodium polytungstate) separations. The quartz was etched by 48 percent HF for 50 minutes to dissolve any remaining feldspar grains that may be present in the quartz separate and to remove the alpha-irradiated layer around the surface of the grains. At each stage of the separation procedures, samples were generously rinsed with distilled water.

The quartz OSL measurements were measured using Risø TL/OSL-DA-15 reader (Bøtter-Jensen *et al.*, 2000). Samples were irradiated using standard sealed $^{90}\text{Sr}/^{90}\text{Y}$ beta sources, calibrated against known γ irradiated samples over a range of grain sizes from 5 to 200 μm (Armitage and Bailey, 2005). The ultraviolet OSL emissions were detected by Electron Tubes bialkaline photomultiplier tube (PMT) EMI-9235QA fitted with Hoya U-340 filters. All OSL measurements were made using 10 mm diameter aluminium discs onto which a 5 mm diameter spot was sprayed in the centre with “Silkospray” silicone oil. A monolayer of several hundred grains was adhered to the surface of each disc to form an aliquot for

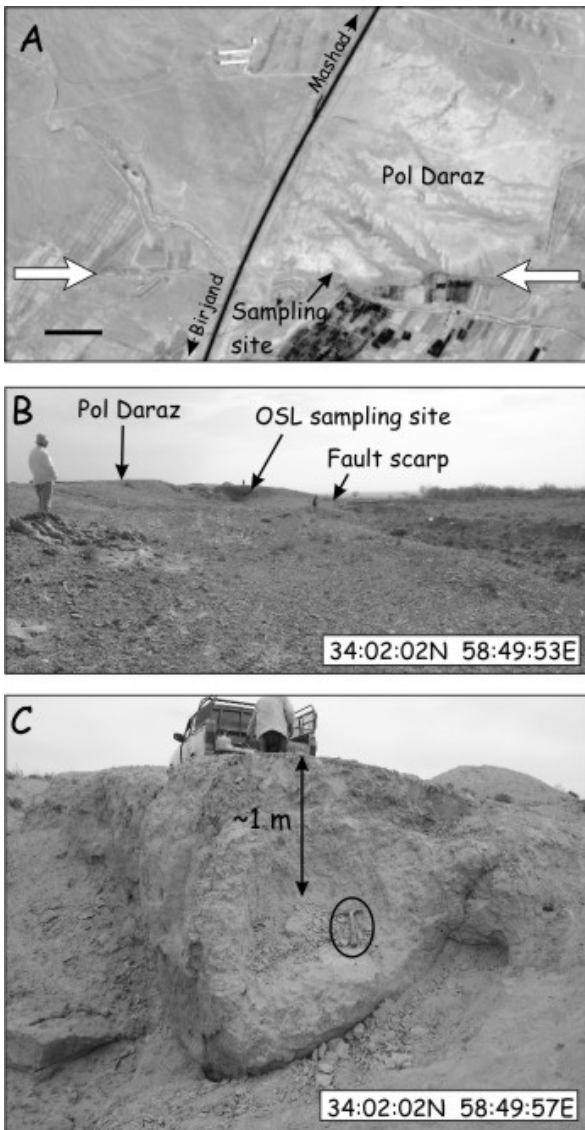


Fig. 4. (a) High-resolution Quickbird satellite imagery (from GoogleEarth; <http://earth.google.com/>) showing Pol Daraz; a region of localised uplift across the Dasht-e-Bayaz fault. The OSL sampling site is labelled. sample DB2 has been collected ~150 m to the east of sample DB1. (b) Photograph looking east along the Dasht-e-Bayaz fault at Pol Daraz. The DB1 OSL sample was taken from the wall of a small excavation into the scarp. (c) Photograph showing lake-bed sediments exposed at the OSL sampling location. DB1 as a single block of lake-bed sediments (roughly 30 cm on each side) was extracted from the exposure just to the left of the geological hammer (circled). The sample was ~1.25 m below the land surface.

measurement. The quartz grains were then dated using the single aliquot regenerative-dose (SAR) protocol (Table 1).

Single Aliquot Regenerative-dose (SAR) (Murray and Wintle, 2000) uses the luminescence signal from a test dose administered after the regeneration dose luminescence measurement to monitor, and then correct for, any sample sensitivity changes during the measurement process. The fundamental assumption in SAR protocol is

that if a plot of regeneration dose OSL (L_x) vs. test dose OSL (T_x) shows a straight line for repeated application of the same dose that passes through the origin, the sensitivity-correction procedure has worked properly. We checked sensitivity changes of the quartz extract of the sample by repeated (8 times) cycles in SAR procedure with a repeated fixed regeneration and test dose. It showed a linear relationship which passed through the origin.

To investigate the saturation of luminescence signal the SAR protocol using 9 different regenerative doses were performed. It is clear from Fig. 5 that a natural dose of > 100 Gy could be accurately measured before saturation occurs. To test thermal transfer of charge into the OSL traps as a result of preheating (e.g. Rhodes, 2000), the natural aliquots were stimulated at room temperature and OSL was measured for 100 sec, with more than 4 hours delay between stimulation (to empty the rapidly

Table 1. Generalized single aliquot regenerated sequence and outline of the steps involved in the SAR method. *Observed L_x and T_x are derived from the initial OSL signal (2 s) minus a background estimated from the last part of the stimulation curve (10 s). Corrected natural signal $N = L_0/T_0$; Corrected regenerated signal $R_x = L_x/T_x$ ($x = 1-5$). Note that in step 2, the sample has been heated to the pre-heat temperature using TL and held at that temperature for 10 s.

Step	Treatment 1	*Ob
1	Beta dose	–
2	Pre-heat (TL 200–300°C for 10 s)	–
3	OSL Stimulation (at 120°C for 100 s)	L_x
4	Beta test dose	–
5	Cut-heat (TL 120–260°C for 10 s)	–
6	OSL Stimulation (at 125°C for 100 s)	T_x
7	Return to 1	–

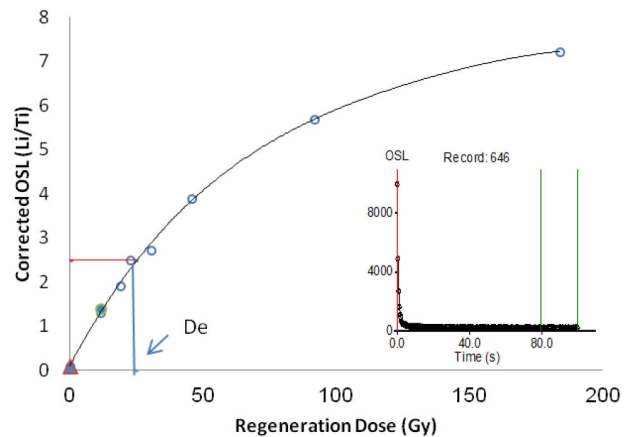


Fig. 5. Growth curve with Natural OSL decay curve. The first regenerative dose was repeated at the end of measurement (filled circle). Recuperation is close to zero and is shown as filled triangle. The test dose was 7 Gy. The natural OSL decay curve is shown inset. Error bars are too small to show.

bleaching test). Very low OSL signal (2% of the natural) was observed for the second measurement. This suggests that thermal transfer is not an effective source of uncertainty in these aliquots.

Dose recovery tests were carried out to provide a method to determine whether the overall effects of sensitivity changes had been properly corrected for. Three aliquots were used for each preheat or cut heat temperature. After depleting the natural signal, each aliquot was given ~ 24.66 Gy of beta dose and this dose was measured using the SAR procedures. The cut heat was first fixed at 220°C for 10 s and the preheat was changes between 200 to 300°C . Then, the preheat was fixed at 260°C and the cut heat varied between 120 – 260°C . The SAR procedure successfully recovered the lab dose at different temperatures (Fig. 6).

The average ratio of observed to given dose for preheat plateau and cut heat plateau was 1.002 ± 0.020 and 1.003 ± 0.036 , respectively. These results showed that the overall effects of sensitivity changes (arising from possible changes in both electron trapping and luminescence recombination probabilities) are corrected. To determine the appropriate thermal pre-treatments in the SAR (Table 1), preheat plateau was carried out. Fig. 7 shows an apparently constant D_e in the temperature range 200 – 300°C with the relevant recycling ratios (R5/R1) close to unity

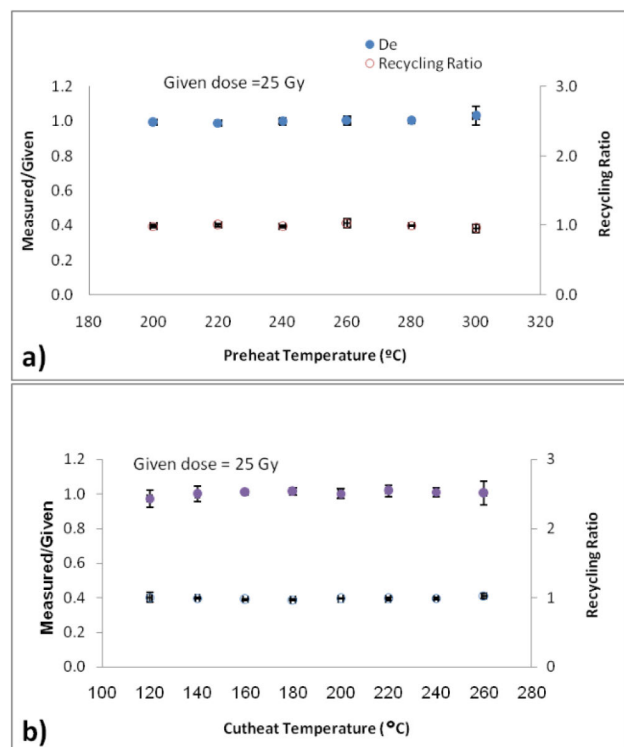


Fig. 6. Dose recovery test. (a) The cut heat was fixed at 220°C and sample temperature was 125°C . (b) The pre heat was fixed at 260°C and sample temperature was 125°C . The ratio of measured to given dose is shown as filled circles and the recycling ratios (R5/R1) at each temperature as open circles. Error bars are too small to show.

(average 1.036 ± 0.036). Based on the above experiments a preheat temperature of 260°C (step 2 in Table 1) and a cut heat of 220°C (step 5 in Table 1) were selected for D_e determination.

Twenty three and twenty six medium size aliquots of samples, DB1 and DB2 respectively, were prepared and measured using the optimised SAR protocol. Following measurement of the naturally acquired dose, a dose-response curve was constructed from five dose points including three regenerative doses (8, 16, and 26 Gy), and a zero dose. A replicate measurement of the lowest regenerative dose was carried out at the end of each SAR cycle. The first 2 seconds of the OSL decay curve was used for the signal, and the final 15 s of the OSL decay curve was used as a background for all measurements. The D_e was determined by interpolation and the sensitivity was corrected by dividing L_x by T_x .

No aliquot produced significant recuperation signals and all produced recycling ratios between 0.90 and 1.10. Fig. 8 shows the equivalent dose measurement, which is the total radiation dose, required to replicate the natural OSL signal. The D_e calculated by central age model for samples DB1 and DB2 are 24.3 ± 0.6 Gy and 20.2 ± 1.8 Gy, respectively.

The dose rate was calculated from ICP mass spectrometer measurements of U, Th, and ICP-AES K for sample DB1. The dose rate for sample DB2 was calculated from data acquired by field gamma spectrometry. Full preparatory and analytical procedures are described by Fattahi *et al.* (2006). The total dose rate (from U, Th, and ^{40}K content and corrections for cosmic ray and moisture contents) was calculated and presented in Table 2.

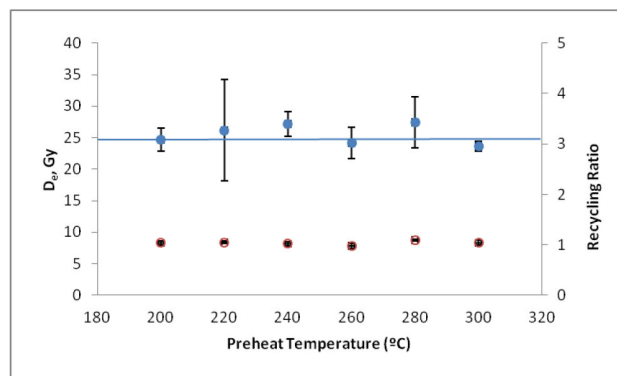


Fig. 7. Plot of equivalent dose as a function of preheat temperature. The cut heat was fixed at 220°C and sample temperature was 125°C . The line is presented to show the accepted value of D_e (24.7 ± 2.7 Gy) for age determination. The scattering of D_e measured for each preheat temperature is shown by large variability in the error bars. The Equivalent dose are shown as filled circles and the recycling ratios (R5/R1) of each temperature as open circles.

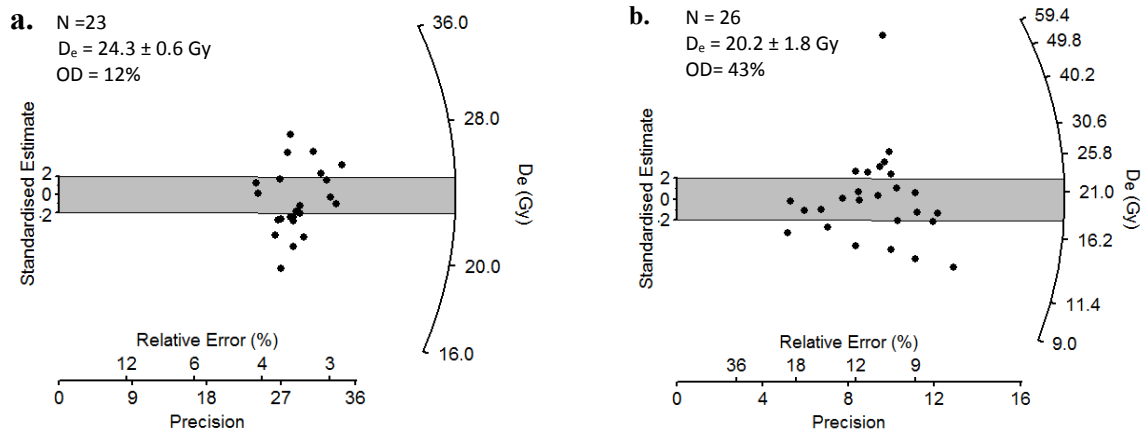


Fig. 8. Radial plot dose distribution diagrams for quartz grains. a. DB1 and b. DB2 samples, respectively. *N* is the number of aliquots, OD is the Overdispersion.

Table 2. Values used to calculate luminescence ages from Dasht-e-Bayaz, NE Iran. Central age model was used for D_e determination. Average water content was estimated as 5%. 23 of 26 aliquots passed the SAR criteria.

Sample	Grain size (μm)	Water (%)	Depth (m)	K (%)	U (ppm)	Th (ppm)	Cosmic (Gy/ka)	Dose rate (mGy/yr)	D_e (Gy/ka)	Age (ka)
DB1	90–150	5	1.25	1.42 ± 0.01	3.2 ± 0.01	7.20 ± 0.01	0.21 ± 0.13	2.82 ± 0.16	24.3 ± 0.6	8.6 ± 0.6
DB2	90–150	5	1.5	1.27 ± 0.01	2.03 ± 0.1	6.88 ± 0.1	0.22 ± 0.13	2.38 ± 0.15	20.2 ± 1.8	8.5 ± 1.0

Slip-rate estimate

We now have a measurement of 26 ± 2 m of cumulative fault slip since abandonment of the Nimbluk dry lake. We also have OSL age determination of 8.6 ± 0.6 and 8.5 ± 1.0 ka for lake-bed deposits from 1.25 and 1.5 m below the surface. Combining the minimum cumulative offset of 24 m by the oldest possible age of sample DB1 (9.2 ka) provides a minimum bound on the slip rate of 2.6 mm/yr. Similarly, dividing the minimum offset of 24 m by the oldest possible age of sample DB2 (9.5 ka) provides another minimum bound on the slip rate of 2.52 mm/yr. Therefore, one has to retain 2.6 mm/yr (the larger value of the two minimum estimates) as a safe minimum slip rate. This minimum right-slip rate remains constant with the previously proposed Holocene slip rate of 2.5 mm/yr by Berberian and Yeats (1999a). In addition, the minimum slip rate of 2.6 mm/yr remains within the range of the Holocene slip rate of 2.4 ± 0.3 mm/yr estimated before on the central section of the Doruneh fault by Fattahi *et al.* (2007).

However, we really don't know when the abandonment occurred relative to the deposition of the fine deposits. The lake-bed surface could have been at grade for some time, so there could be a lag time between the deposition of the lake-bed sediments and the actual incision. Since the 26 ± 2 m offset is incised into the surface, we don't really have a complete link between the deposit and the time of the incision. We also do not know whether the

26 ± 2 m of stream displacement represents the total fault displacement since desiccation of the palaeo-lake.

4. IMPLICATIONS FOR THE SEISMIC HAZARD AND ACTIVE TECTONICS OF IRAN

The Dasht-e-Bayaz fault appears to have a minimum slip-rate, averaged over the Holocene, which is at least 2.6 mm/yr which is the only quantitative constraint on the slip-rate of the Dasht-e-Bayaz fault.

A maximum of 4.5 m of left-lateral slip was measured in the 1968 earthquake and an average displacement of 2.5 m (Ambraseys and Tchalenko, 1969). Using the minimum slip rate of 2.6 mm/yr, the maximum slip of 4.5 m and the average slip of 2.5 m would accumulate roughly in about 1700 and 1000 years, respectively. Ruptures from the 1979 earthquake were not investigated in great detail but values of 1 m to 4 m were recorded (Haghipour and Amidi, 1980).

The relatively rapid rate of slip on the Dasht-e-Bayaz fault, and consequently the rather short likely return period for earthquakes such as those in 1968 event and 1979 event, may help to explain the high rate of historical earthquakes recorded around Dasht-e-Bayaz (e.g., Ambraseys and Melville, 1982; Berberian and Yeats, 1999a, Walker *et al.*, 2004). However, none of the pre-twentieth century events can be assigned to any individual fault with certainty.

The slip-rate of the Dasht-e-Bayaz fault has implications for the active tectonics of Iran. Walker *et al.* (2004) suggest that the eastern part of the Doruneh fault (Fig. 1b) has rotated clockwise about a vertical axis until it has achieved an orientation that is perpendicular to the regional direction of shortening, at which point it can no longer rotate, and so can no longer accommodate the regional north-south right-lateral shear. The Dasht-e-Bayaz fault, which has only small amounts (5–6 km) of cumulative slip and a subdued appearance in the topography, was then initiated at the expense of the Doruneh fault. Our minimum estimate of 2.6 mm/yr for the slip-rate of the Dasht-e-Bayaz fault remains within the range of Holocene slip rate of 2.4 ± 0.3 mm/yr estimated before on the central section of the Doruneh fault.

5. CONCLUSION

The Dasht-e-Bayaz fault, which has been responsible for two destructive earthquakes of Mw 7.1 in 1968 and 1979, has a slip-rate of at least 2.6 mm/yr. The maximum of 4.5 m of left-lateral slip in the 1968 earthquake would accumulate in 1700 years, and the average displacement of 2.5 m would accumulate in ~1000 years. The slip-rate we estimate for the Dasht-e-Bayaz fault remains within the range of Holocene slip rate of 2.4 ± 0.3 mm/yr for the adjacent Doruneh fault (Fattahi *et al.*, 2007).

ACKNOWLEDGEMENTS

We would like to thank the University of Oxford, the University of Tehran, the Geological Survey of Iran and the University of Birjand for their support of our work in Iran. The project was funded by the Leverhulme Trust (award number RNUB0, project number ACRNUB0). MF travel to Oxford is supported by grant no 6201002/1/10 awarded by Tehran University. MF Would like to thank G G Nejad for general supports, without it he could not carry on his research.

REFERENCES

- Ambraseys NN and Melville CP, 1982. *A history of Persian earthquakes*. Cambridge University Press, UK.
- Ambraseys NN and Tchalenko JS, 1969. The Dasht-e-Bayaz (Iran) earthquake of August 31, 1968: a field report. *Bulletin of the Seismological Society of America* 59: 1751–1792.
- Armitage SJ and Bailey RM, 2005. The measured dependence of laboratory beta dose rates on sample grain size. *Radiation Measurements* 39: 123–127, DOI 10.1016/j.radmeas.2004.06.008.
- Berberian M, 1976. *Contribution to the seismotectonics of Iran (Part II)*. Report No. 39. Geological Survey of Iran.
- Berberian M and Yeats RS, 1999a. Patterns of historical earthquake rupture in the Iranian Plateau. *Bulletin of the Seismological Society of America* 89: 120–139.
- Berberian M and Yeats RS, 1999b. Contribution of archaeological data to studies of earthquake history in the Iranian Plateau. *Journal of Structural Geology* 23: 563–584, DOI 10.1016/S0191-8141(00)00115-2.
- Berberian M, Jackson JA, Qorashi M, Khatib MM, Priestley K, Talebian M and Ghafuri-Ashtiani M, 1999. The 1997 May 10 Zirkuh (Qa'nat) earthquake (Mw 7.2): faulting along the Sistan suture zone of eastern Iran. *Geophysical Journal International* 136: 671–694, DOI 10.1046/j.1365-246x.1999.00762.x.
- Bøtter-Jensen L, Bulur E, Duller GAT and Murray AS, 2000. Advances in luminescence instrument systems. *Radiation Measurements* 32: 523–528, DOI 10.1016/S1350-4487(00)00039-1.
- Engdahl ER, van der Hilst R and Buland R, 1998. Global teleseismic earthquake relocation with improved travel times and procedures for depth determination. *Bulletin of the Seismological Society of America* 88: 722–743.
- Farr TG and Kobrick M, 2000. Shuttle Radar Topography Mission produces a wealth of data. *Eos, Transactions American Geophysical Union* 81: 583–585, DOI 10.1029/EO081i048p00583.
- Fattahi M, Walker R, Hollingsworth J, Bahroudi A, Nazari H, Talebian M, Armitage S, and Stokes S, 2006. Holocene slip-rate on the Sabzevar thrust fault, NE Iran, determined using optically stimulated luminescence (OSL). *Earth and Planetary Science Letters* 245: 673–684, DOI 10.1016/j.epsl.2006.03.027.
- Fattahi M, Walker RT, Khatib MM, Dolati A and Bahroudi A, 2007. Slip-rate estimate and past earthquakes on the Doruneh fault, eastern Iran. *Geophysical Journal International* 168: 691–709, DOI 10.1111/j.1365-246X.2006.03248.x.
- Haghipour A and Amidi M, 1980. Geotectonics of the Ghaenat earthquakes of NE Iran (Nov 14th to Dec. 9. 1979). *Bulletin of the Seismological Society of America* 70: 1751–1757.
- Jackson J, 2001. Living with earthquakes: know your faults. *Journal of Earthquake Engineering* 5(Supplement 001): 5–123, DOI 10.1080/13632460109350530.
- Jackson J and McKenzie D, 1984. Active tectonics of the Alpine-Himalayan belt between Turkey and Pakistan. *Geophysical Journal of the Royal Astronomical Society* 77: 185–264, DOI 10.1111/j.1365-246X.1984.tb01931.x.
- Meyer B and Le Dortz K, 2007. Strike-slip kinematics in Central and Eastern Iran: estimating fault slip-rates averaged over the Holocene. *Tectonics* 26: TC5009, DOI 10.1029/2006TC002073.
- Murray AS and Wintle AG, 2000. Luminescence dating of quartz using an improved single-aliquot regenerative-dose protocol. *Radiation Measurements* 32: 57–73, DOI 10.1016/S1350-4487(99)00253-X.
- Nowroozi AA and Mohajer-Ashjai A, 1980. Faulting of Kurizan and Koli (Qaenat Iran) earthquakes of November 1979: a field report. *Iranian Petroleum Institute Bulletin* 78: 8–20.
- Ritz J-F, Brown E, Bourles D, Philip H, Schlupp A, Raisbeck G, Yiou F and Enkhtuvshin B, 1995. Slip rates along active faults estimated with cosmic-ray exposure dates: applications to the Bogd fault, Gobi-Altai, Mongolia. *Geology* 23: 1019–1022, DOI 10.1130/0091-7613(1995)023<1019:SRAAFE>2.3.CO;2.
- Rhodes E, 2000. Observations of thermal transfer OSL signals in glaciogenic quartz. *Radiation Measurements* 32: 595–602, DOI 10.1016/S1350-4487(00)00125-6.
- Tchalenko JS and Ambraseys NN, 1970. Structural analysis of the Dasht-e-Bayaz (Iran) earthquake fractures. *Geological Society of America Bulletin* 81: 41–60.
- Tchalenko JS and Berberian M, 1975. Dasht-e-Bayaz fault, Iran: Earthquake and earlier related structures in bed-rock. *Geological Society of America Bulletin* 86: 703–709.
- Van der Woerd J, Klinger Y, Sieh K, Tapponnier P, Ryerson FJ and Mériaux AS, 2006. Long-term slip rate of the southern San Andreas fault, from ¹⁰Be-²⁶Al surface exposure dating of an offset alluvial fan. *Journal of Geophysical Research: Solid Earth*: 111: B04407, DOI 10.1029/2004JB003559.
- Vernant P, Nilforoushan F, Hatzfeld D, Abassi MR, Vigny C, Masson F, Nankali H, Martinod J, Ashtiani A, Bayer R, Tavakoli F and Chery J, 2004. Present-day crustal deformation and plate kinematics in the Middle East constrained by GPS measurements in Iran and northern Oman. *Geophysical Journal International* 157: 381–398, DOI 10.1111/j.1365-246X.2004.02222.x.
- Walker R and Jackson J, 2004. Active tectonics and late Cenozoic strain distribution in central and eastern Iran. *Tectonics* 23: TC5010, DOI 10.1029/2003TC001529.

- Walker R, Jackson J and Baker C, 2004. Active faulting and seismicity of the Dasht-e-Bayaz region, eastern Iran. *Geophysical Journal International* 157: 265–282, DOI 10.1111/j.1365-2966.2004.02179.x.
- Walker RT, Bergman EA, Szeliga W and Fielding EJ, 2011. Insights into the 1968–1997 Dasht-e-Bayaz and Zirkuh earthquake sequences, eastern Iran, from calibrated relocations, InSAR and high-resolution satellite imagery. *Geophysical Journal International* 187: 1577–1603, DOI 10.1111/j.1365-246X.2011.05213.x.
- Walpersdorf A, Manighetti I, Mousavi Z, Tavakoli F, Vergnolle M, Jadidi A, Hatzfeld D, Aghamohammadi A, Bigot A, Djamour Y, Nankali H and Sedighi M, 2014. Present-day kinematics and fault slip rates in eastern Iran, derived from 11 years of GPS data. *Journal of Geophysical Research: Solid Earth* 119: 1359–1383, DOI 10.1002/2013JB010620.